

Effect of Multiple Metal Substitutions for A- and B-perovskite Sites on the Thermoelectric Properties of LaCoO₃

S. Harizanova¹, E. Zhecheva¹, V. Valchev², P. Markov¹, M. Khristov¹, R. Stoyanova^{1*}

¹Institute of General and Inorganic Chemistry, Bulgarian Academy of Sciences, 1113 Sofia, Bulgaria

²Faculty of Physics, University of Sofia, 1164 Sofia, Bulgaria

ABSTRACT

The present contribution provides new data on the effect of multiple metal substitutions for A- and B-perovskite sites on the thermoelectric properties of LaCoO₃-based ceramics. Two groups of perovskite compositions are studied: double substituted cobaltates with general formula LaCo_{0.8}M_{0.1}M'_{0.1}O₃ (M_{0.1}M'_{0.1} ≡ Ni_{0.1}Fe_{0.1}, Ni_{0.1}Ti_{0.1}, Mn_{0.1}Fe_{0.1}) and Sr-containing cobaltate with La_{0.9}Sr_{0.1}Co_{0.8}Ni_{0.1}Fe_{0.1}O₃. The content of all magnetic (Ni, Fe and Mn) and diamagnetic (Ti and Sr) elements are chosen to be 0.10 mol. Structural and morphological characterizations are carried out by powder XRD, SEM and TEM analyses. The thermoelectric efficiency of the perovskites is determined by the dimensionless figure of merit, calculated from the independently measured Seebeck coefficient, electrical resistivity and thermal conductivity. The effectiveness of the multiple metal substitutions for improvement of the thermoelectric properties of LaCoO₃-based ceramics is discussed.

Keywords: Cobalt-Based Perovskites; Thermoelectric Oxides.

I. INTRODUCTION

A basic concept of thermoelectric materials is their ability to convert heat into electricity [1]. The thermoelectric efficiency is evaluated by the dimensionless figure-of-merit: $ZT = S^2 \sigma T / k$ where S is the Seebeck coefficient, σ and k denote electrical and thermal conductivity. Therefore, large Seebeck coefficient, large electrical conductivity and low thermal conductivity are simultaneously required to achieve high thermoelectric efficiency. As these three physical parameters are interrelated, developing of thermoelectric materials represents a scientific challenge [2]. That is why after a period of intensive studies performed in 1950-1960 the interest in such studies faded. But the research interest in these materials resurrected after 1997, the experimental finding of Terasaki [3] on layered sodium cobalt oxides having large thermopower contributing to this.

As a result of intensive studies, both cobalt-based sulfides and oxides are considered as most suitable thermoelectric materials [4]. The more covalent character of the chemical bond for sulfides is responsible for their larger power factor even at room temperature.

However, cobalt-based sulfides display poor chemical and physical stability under high temperatures and oxidizing conditions in comparison with that for oxides. Among oxides, three groups of cobaltates can be outlined: Na_xCoO₂ with a layered structure; misfit Ca₃Co₄O₉, with similar CoO₂ layers and LaCoO₃ with a perovskite structure. LaCoO₃ is one of the most interesting as a material with potential application in thermoelectricity due to its high Seebeck coefficient ($|S| > 500 \mu\text{V/K}$ at room temperature) [5]. The transport properties of LaCoO₃ are determined (to a great extent) by the ability of Co³⁺ ions to adopt low-, intermediate- and high-spin configurations in the perovskite structure, leading to an additional spin entropy effect [6,7]. However, the electrical resistivity is high (about 10 Ωcm at room temperature), which lowers the thermoelectric activity ($ZT < 0.01$ at $T = 300$ K). Therefore, the state-of-the-art research is mainly devoted to the enhancement of the thermoelectric efficiency of LaCoO₃ by single substitution for the La- and Co-sites [8,9].

Recently, we have demonstrated that multiple substitutions of Ni and Fe for Co in LaCo_{1-x-y}Ni_xFe_yO₃ is a more effective way to improve its thermoelectric efficiency in comparison with single-substituted

analogues $\text{LaCo}_{1-x}\text{Ni}_x\text{O}_3$ and $\text{LaCo}_{1-x}\text{Fe}_x\text{O}_3$ [10]. This is a result from the synergic effect of Ni and Fe leading to a drastic reduction of the thermal conductivity.

The aim of this contribution is to improve the thermoelectric properties of LaCoO_3 -based ceramics by extending our studies on the effect of multiple metal substitutions on both La and Co-sites. Two groups of perovskite compositions are studied: double substituted cobaltates with general formula $\text{LaCo}_{0.8}\text{M}_{0.1}\text{M}'_{0.1}\text{O}_3$ ($\text{M}_{0.1}\text{M}'_{0.1} \equiv \text{Ni}_{0.1}\text{Fe}_{0.1}, \text{Ni}_{0.1}\text{Ti}_{0.1}, \text{Mn}_{0.1}\text{Fe}_{0.1}$) and Sr-containing cobaltate with $\text{La}_{0.9}\text{Sr}_{0.1}\text{Co}_{0.8}\text{Ni}_{0.1}\text{Fe}_{0.1}\text{O}_3$. The content of all magnetic (Ni, Fe and Mn) and diamagnetic (Ti and Sr) elements are chosen to be 0.10 mol. Structural and morphological characterizations are carried out by powder XRD, SEM and TEM analyses. The thermoelectric efficiency of the perovskites is determined by the dimensionless figure of merit, calculated from the independently measured Seebeck coefficient (S), electrical resistivity (ρ) and thermal conductivity (λ).

II. METHODS AND MATERIAL

A. Synthesis Method

Multiple-substituted cobaltates were prepared by a precursor-based method, where citric acid is used as a complexation agent. The procedure is described elsewhere [10,11]. Homogenous $\text{La}_{1-y}\text{Sr}_y\text{Co}_{1-x}\text{M}_x\text{O}_3$ ($\text{M}=\text{Ni}, \text{Fe}$) citrate precursors were obtained by freeze drying. Mixed lanthanum-cobalt-metal (Ni, Fe, Sr) citrates were prepared by adding a 5 M aqueous solution of citric acid (CA) to a suspension of CoCO_3 - NiCO_3 - $\text{Fe}(\text{NO}_3)_3$ - SrCO_3 in aqueous solution of $\text{La}(\text{NO}_3)_3 \cdot 6\text{H}_2\text{O}$ (1M La). The ratio between the components was $(\text{La}_{0.9}\text{Sr}_{0.1}):(\text{Co}_{0.8}\text{Ni}_{0.1}\text{Fe}_{0.1}): \text{CA} = 1:1:10$. After stirring, a clear solution was obtained, which was diluted to 0.25M La ($\text{Co}_{1-x}\text{M}_x$). The solution was frozen instantly with liquid nitrogen and dried under vacuum (20–30 mbars) at -20°C in an Alpha-Christ Freeze-Dryer. For the preparation of $\text{LaCo}_{0.8}\text{Ti}_{0.1}\text{Ni}_{0.1}\text{O}_3$ and $\text{LaCo}_{0.8}\text{Mn}_{0.1}\text{Fe}_{0.1}\text{O}_3$ compositions, a modified Pechini-type method is applied. The solution containing CoCO_3 , NiCO_3 , TiO_2 , $\text{Mn}(\text{CH}_3\text{COO})_2$, $\text{Fe}(\text{NO}_3)_3$ and citric acid in an appropriate ration was heated up to $\sim 90^\circ\text{C}$ and ethylene glycol (EG) was added (CA:EG=1:4). The solution thus obtained was continuously stirred with a

magnetic stirrer on a hot plate to remove the excess of water and to accomplish the polyesterification reaction. Prolonged heating produced a more and more viscous and bubbly mass.

The thermal decomposition of all precursors was achieved at 400°C for 3 h in air. The obtained solid residue was annealed at 800°C for 20 h in air. Finally, the powders were sintered at 900°C for 40 h in air, then cooled down to room temperature with a rate of $5^\circ/\text{min}$.

B. Methods of Characterization:

X-ray structural analysis was performed on a Bruker Advance 8 diffractometer with $\text{Cu K}\alpha$ radiation. Step-scan recordings for structure refinement by the Rietveld method were carried out using $0.02^\circ 2\theta$ steps of 5 s duration. XRD patterns are analyzed by a structural model comprising rhombohedrally distorted perovskite-type structure ($R\bar{3}c$ space group) where La occupies the $6a$ position (0, 0, 1/4), Co/Fe/Ni are in the octahedral $6b$ position, and oxygen is in the $18e$ position. Determination of occupancy factors in these systems is a complicated procedure, as demonstrated by neutron diffraction studies on single-substituted perovskites [12]. In order to simplify the fitting procedure the total occupancy of La on $6a$ sites and Co/Ni on $6b$ sites was constrained to 1/6. Details of the fitting procedure are given elsewhere [10,12]. It is important that the procedure suitable for describing the cationic distribution in $\text{LaCo}_{1-x}\text{Ni}_x\text{O}_3$ is also applicable for the $\text{LaCo}_{1-x}\text{Fe}_x\text{O}_3$ series [12]. Irrespective of the uncertainty in the Rietveld refinement model for determination of the oxygen content, the results give evidence that the oxygen deficiency for iron- substituted perovskites (i.e., both $\text{LaFe}_y\text{Ni}_x\text{Co}_{1-x-y}\text{O}_3$) is limited and close to 3 (Table 1). This is in agreement with our previous data on hydrogen reduction of $\text{LaCo}_{1-x}\text{Fe}_x\text{O}_3$ [12].

SEM images of pellets coated with gold were obtained by a Zeiss DSM 962 microscope and Philips XL30 scanning electron microscope. TEM observations were obtained using a JEOL 2100 transmission electron microscope, operating at 200 kV, and equipped with a double tilt holder. The powder was first crushed in alcohol in an agate mortar, ultrasonicated for 360 seconds and then a drop of the suspension was deposited and dried on a copper grid coated with a thin film of

amorphous carbon. The measurements of lattice-fringe spacing recorded in HRTEM micrographs were made using digital image analysis of reciprocal space parameters. The analysis was carried out by the Digital Micrograph software.

The transport properties were measured on pellets sintered at 900 °C for 40h. This temperature was chosen in order to avoid the disproportionate of the iron-rich cobaltates when heated at $T > 900$ °C. SEM analysis was undertaken to analyze the pellet porosity. Electrical resistivity, density and mobility of charge carriers were determined by a MMR's Variable Temperature Hall System (K2500-5SLP-SP) using the Van der Pauw method over a temperature range from 90 to 600 K. The bench top permanent magnet (5 T) is used.

Thermal conductivity was determined at room temperature on a Thermal Conductivity Analyzer TCi (SETARAM). In order to compare the thermal conductivities of samples having different pellet porosity, the thermal conductivity is normalized to 95% of the theoretical density (λ_t) using the following density correction [13]: $\lambda_t = \lambda(0.95^{1.5})/(1-P)^{1.5}$, where λ is the measured thermal conductivity and P is the fractional porosity of the pellet.

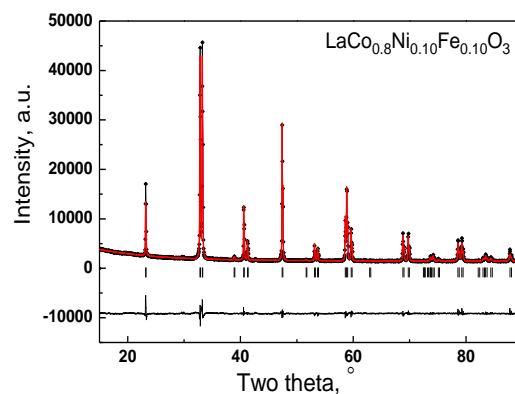
III. RESULT AND DISCUSSION

A. Structure of Multiple Metal Substituted Perovskites

XRD patterns of double substituted perovskites are shown on Figure 1. All diffraction patterns are indexed in the framework of R-3c structural model, where La^{3+} ion occupies (0, 0, 0.25) position, transition metal ions are randomly distributed over (0, 0, 0) position and O^{2-} ion is in (x_0 , 0, 0.25) site. The calculated structural parameters are listed in Table 1. The substitution of Sr^{2+} for La^{3+} in $\text{La}_{1-y}\text{Sr}_y\text{Co}_{1-x}(\text{Ni}_{0.5}\text{Fe}_{0.5})_x\text{O}_3$ is also accomplished in the framework of the rhombohedrally distorted perovskite-type structure (Table 1). The replacement of Co ions by (Mn+Fe), (Ti+Ni) and (Ni+Fe) pairs leads to a lattice expansion. In addition, the lattice expansion is also observed when aliovalent Sr^{2+} ions substituted for La^{3+} ions. The analysis of structural parameters reveals that simultaneous occurrence of (Mn+Fe) and (Ni+Fe) pairs into perovskite structure causes a local elongation of the

mean bond lengths $\text{La-Co}_{1-x}\text{M}_x$ and $\text{Co}_{1-x}\text{M}_x\text{-O}$ without changing the extent of rhombohedral distortion (expressed by $\text{Co}_{1-x}\text{M}_x\text{-O-Co}_{1-x}\text{M}_x$ angle, Table 1). Contrary, the (Ti+Ni) pair reduces significantly the local rhombohedral distortion together with an increase of the mean $\text{La-Co}_{1-x}\text{M}_x$ bond distance, while the mean $\text{Co}_{1-x}\text{M}_x\text{-O}$ bond length remains nearly unchanged. A reduction in the local rhombohedral distortion is also observed when Sr^{2+} ions substitute for La^{3+} in LaCoO_3 (Table 1).

In the case of the (Ni+Fe) and Sr-containing systems, a small oxygen deficiency is established (i.e. $\text{La}_{1-y}\text{Sr}_y\text{Co}_{1-x}\text{M}_x\text{O}_{3-\delta}$). It is worth mentioning that the oxygen deficiency is a typical phenomenon for single substituted cobaltates with nickel and strontium [14-16]. The compensation of the oxygen deficiency in $\text{LaCo}_{1-x}\text{Ni}_x\text{O}_3$ has been achieved through stabilization of Ni^{2+} ions instead of Co^{2+} ions [12], while highly oxidized Co^{4+} ions due to their limited thermal stability compensate partially the Sr^{2+} charges. The Ni^{2+} ion exhibits a larger ionic dimension (0.69 Å, respectively) in comparison with that for low- and high-spin Co^{3+} and Ni^{3+} ions, leading to an increase in the lattice parameters upon Ni substitution. The ionic radius of Sr^{2+} is sufficiently larger in comparison with that for La^{3+} so that it compensates the appearance of smaller Co^{4+} ions. This allows us to relate the oxygen deficiency in (Ni+Fe)- and Sr-substituted perovskites to the Ni and Sr elements (Table 1). In comparison with Ni and Sr, Mn-containing perovskites are able to accommodate extra oxygen, as a result of which $\text{LaMnO}_{3+\delta}$ is stabilized [17]. However, the Rietveld refinement does not give any measurable extra oxygen content for (Mn+Fe) double substituted perovskites. Therefore, the structural analysis reveals that (Mn+Fe) and (Ni+Ti) substituted perovskites are stoichiometric with respect to oxygen.



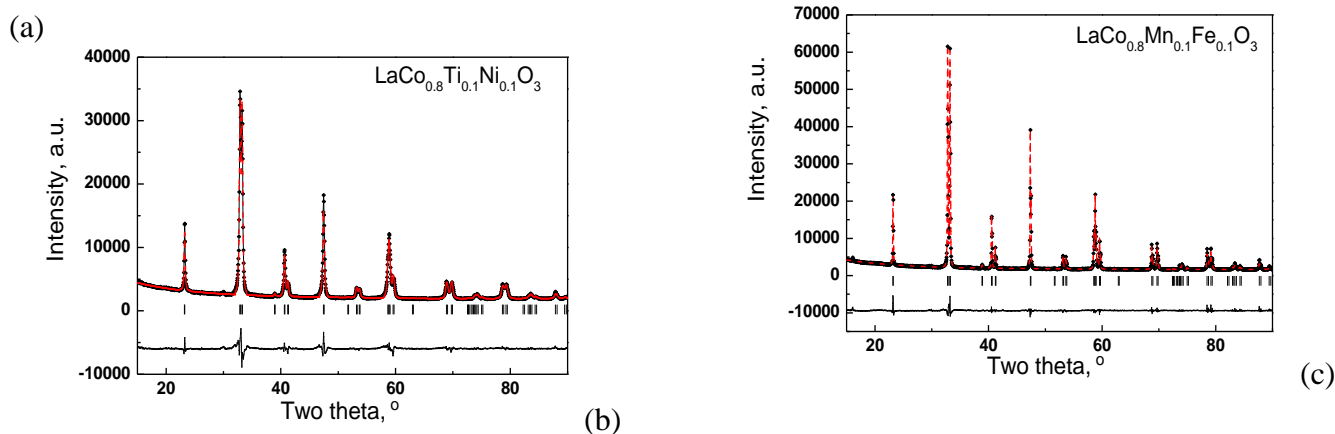


Figure 1: XRD patterns of $\text{LaCo}_{0.8}\text{Ni}_{0.1}\text{Fe}_{0.1}\text{O}_3$ (a), $\text{LaCo}_{0.8}\text{Ti}_{0.1}\text{Ni}_{0.1}\text{O}_3$ (b) and $\text{LaCo}_{0.8}\text{Mn}_{0.1}\text{Fe}_{0.1}\text{O}_3$ (c).

TABLE I

LATTICE PARAMETERS (A AND C), LATTICE VOLUME (V), AVERAGE CO-O BOND LENGTH, CO-O-CO BOND ANGLE, AVERAGE CO-LA DISTANCE, OXYGEN CONTENT (δ), OXYGEN PARAMETER AND R-BRAGG COEFFICIENT FOR MULTIPLE SUBSTITUTED COBALTATES.

| Sample | Lattice parameters | | | Co-O, Å | Co-O-Co, ° | Co-La, Å | $\delta \pm 0.009$ | $x_o \pm 0.0011$ | R_{Br} |
|---|--------------------------|--------------------------|-----------------|---------|------------|----------|--------------------|------------------|-----------------|
| | $a \pm 0.0001, \text{Å}$ | $c \pm 0.0003, \text{Å}$ | $V, \text{Å}^3$ | | | | | | |
| LaCoO_3 | 5.4407 | 13.0914 | 335.61 | 1.932 | 163.81 | 3.273 | 0.0 | 0.5500 | 4.89 |
| $\text{LaCo}_{0.8}\text{Ni}_{0.1}\text{Fe}_{0.1}\text{O}_3$ | 5.4532 | 13.1191 | 337.86 | 1.943 | 163.99 | 3.292 | 0.055 | 0.5494 | 2.60 |
| $\text{LaCo}_{0.8}\text{Ti}_{0.1}\text{Ni}_{0.1}\text{O}_3$ | 5.4479 | 13.1344 | 337.60 | 1.930 | 166.09 | 3.330 | 0.0 | 0.5429 | 3.93 |
| $\text{LaCo}_{0.8}\text{Mn}_{0.1}\text{Fe}_{0.1}\text{O}_3$ | 5.4582 | 13.1376 | 338.96 | 1.937 | 164.13 | 3.336 | 0.0 | 0.5499 | 2.39 |
| $\text{La}_{0.9}\text{Sr}_{0.1}\text{Co}_{0.8}\text{Ni}_{0.1}\text{Fe}_{0.1}\text{O}_3$ | 5.4524 | 13.1536 | 338.65 | 1.933 | 165.58 | 3.288 | 0.045 | 0.5445 | 2.56 |

The analysis of local structural parameters indicates that double substituted perovskites bring all features of the single-substituted ones. The dimension mismatch

between the cobalt, nickel, iron, titanium and manganese ions, as well as the oxygen deficiency typical for Sr and Ni-substituted perovskites, are the main factor controlling the lattice expansion upon single substitution on A- and B-sites. Although Sr, La, Fe and Ti ions have stable oxidation states of +2, +3, +3 and +4, all of the rest elements Co, Ni and Mn can adopt a variety of oxidation states: Co^{2+} , Co^{3+} and Co^{4+} ; Ni^{2+} and Ni^{3+} , Mn^{3+} and Mn^{4+} . It is worth mentioning that all elements causes a lattice expansion, while only Ti^{4+} and Sr^{2+} ions provoke a reduction of the local octahedral distortion. Contrary to double substituted cobaltates, it has been found that the single substituted $\text{LaCo}_{1-x}\text{M}_x\text{O}_3$ with Fe, Mn and Ti ions display an orthorhombic type of structure [18-20].

Based on XRD diffraction, rhombohedrally distorted perovskite-type of structure have been established for $\text{LaCo}_{1-x}(\text{Ni}_{0.5}\text{Fe}_{0.5})_x\text{O}_3$ ($x \leq 0.5$). However, Troyanchuk et

al. [20] have been reported a formation of mixtures of orthorhombic and rhombohedral phases when $\text{LaCo}_{1-x}\text{Fe}_x\text{O}_{3+\delta}$ are heated at 1570 K in air. To confirm the stabilization of the rhombohedral perovskite-like structure upon multiple metal substitutions, TEM analysis on $\text{LaCo}_{0.5}\text{Fe}_{0.5}\text{O}_3$ containing higher Fe content is undertaken. Bright field image, SAED and HRTEM of $\text{LaCo}_{0.5}\text{Fe}_{0.5}\text{O}_3$ are shown on Figure 2. Perovskite oxide has well shaped particles with an average size of around 350 nm. SAED along [010] direction corresponds to a rhombohedrally distorted perovskite structure with lattice parameter of $a = 5.447 \text{ Å}$ and $c = 13.108 \text{ Å}$. HRTEM reveals a good crystallinity of the perovskite oxide, where the lattice fingers form (012) planes are clearly resolved. These results confirm the stabilization of the rhombohedrally distorted structure upon metal substitution.

B. Transport Properties of Multiple Metal Substituted Cobaltates.

Pellets porosity: The morphology of cobaltates is a critical parameter in order to fabricate the dense pellets suitable for electrical resistivity measurements. Figure 3

shows the SEM images of pellets fabricated from double substituted perovskites $\text{LaCo}_{0.8}\text{Fe}_{0.1}\text{Ni}_{0.1}\text{O}_3$, $\text{LaCo}_{0.8}\text{Ti}_{0.1}\text{Ni}_{0.1}\text{O}_3$ and $\text{LaCo}_{0.8}\text{Mn}_{0.1}\text{Fe}_{0.1}\text{O}_3$. For all perovskites, relatively dense pellets are formed at 900 °C (around 80-85 % porosity). At higher magnification, well shaped particles closely connected between them are clearly visible. The average particle dimensions are calculated and they are listed in Table 2. The average particle dimensions vary between 0.2 and 0.5 μm and show a dependence on the nature of transition metal ions substituted for cobalt ions. The lowest sizes are observed for the (Ni+Ti)-double substituted cobaltate, while the (Mn+Fe)-double substituted cobaltate displays highest sizes. However, the porosity of all pellets looks like the same due to the close connection between well-shaped individual particles. The similar pellet densities permit to associate the measured thermoelectric efficiencies with intrinsic properties of multiple substituted cobaltates.

TABLE II.

THE CRYSTALLITE SIZE OF OXIDES WAS CALCULATED FROM THE SEM IMAGES.

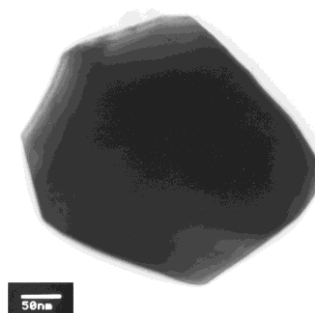
| Samples | $r_{\text{SEM}}, \mu\text{m}$ |
|---|-------------------------------|
| LaCoO_3 | 0.43 ± 0.10 |
| $\text{LaCo}_{0.8}\text{Ni}_{0.1}\text{Fe}_{0.1}\text{O}_3$ | 0.39 ± 0.08 |
| $\text{LaCo}_{0.8}\text{Ti}_{0.1}\text{Ni}_{0.1}\text{O}_3$ | 0.22 ± 0.05 |
| $\text{LaCo}_{0.8}\text{Mn}_{0.1}\text{Fe}_{0.1}\text{O}_3$ | 0.46 ± 0.12 |
| $\text{La}_{0.9}\text{Sr}_{0.1}\text{Co}_{0.8}\text{Ni}_{0.1}\text{Fe}_{0.1}\text{O}_3$ | 0.45 ± 0.10 |

Electrical resistivity. The temperature dependence of the electrical conductivity for multiple substituted cobaltates is given on Figure 4. At 300 K, the electrical resistivity decreases strongly upon double substitution of (Ni+Fe) for Co, while the (Mn+Fe) additives cause an increase in the resistivity (Figure 4).

When Fe ions are replaced by Ti ions, the resistivity for the double substituted (Ni+Ti) cobaltate slightly increases, but it remains lower in comparison with that for unsubstituted cobaltate LaCoO_3 . The most significant decrease in the electrical resistivity of the (Ni+Fe) double substituted cobaltate is achieved when Sr^{2+} ions are added on the A position instead of La^{3+} ions. For all of the samples, the electrical resistivity decreases with raising the temperature from 250 to 600 K, thus

indicating their semiconducting behaviour. The temperature dependence of the electrical resistivity can be calculated by a model based on the nearest neighbor hopping of small polarons: $\rho = \rho_0 T \exp(-E_p/kT)$, where E_p is the polaron hopping energy. For (Mn+Fe), (Ni+Ti) and Sr-substituted cobaltates, the small polaron hopping mechanism is hold in a whole temperature range, while this mechanism is obeyed between 250 and 450 K for the (Ni+Fe)-substituted oxides (Fig. 4). The polaron hopping energy increases in the following order: 0.088 eV, 0.099 eV, 0.120 eV and 0.190 eV for Sr-, (Ni+Fe), (Ni+Ti) and (Mn+Fe) substituted oxides, respectively.

The temperature induced changes in the electrical resistivity and its dependence on the nature of metal ions can be understood taking into account the density and mobility of the charge carriers (Fig. 5, Table 3). On heating from 250 to 600 K, all substituted cobaltates display an increase in both the carrier density and the mobility. The effect of metal ions on the electrical resistivity is consistent with changes in the magnitude of carrier density for LaCoO_3 . Both (Ni+Fe)- and Sr-substituted cobaltates exhibit carrier densities, which are an order of magnitude higher than that for unsubstituted LaCoO_3 (Fig. 5). For double substituted (Ni+Ti) and (Mn+Fe) cobaltates, lower carrier densities are observed. Contrary to the carrier density, the temperature behaviour of the carrier mobility depends on the nature of metal ions



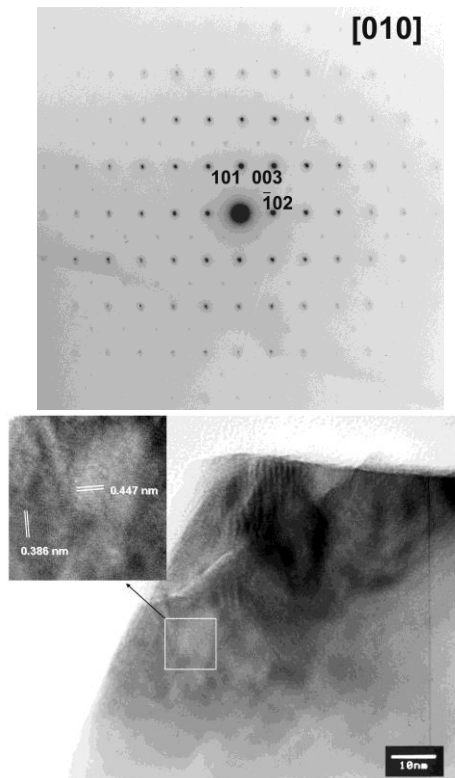
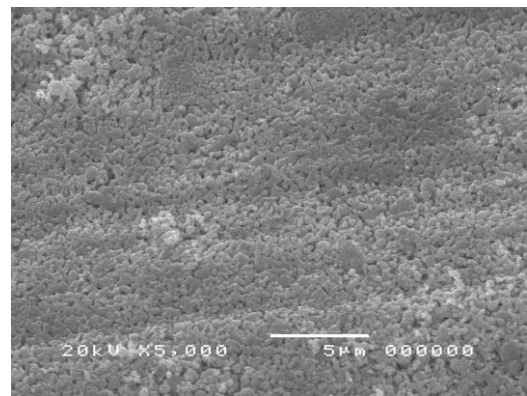
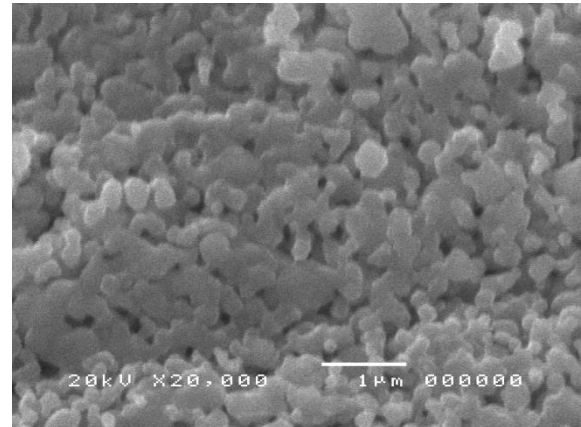


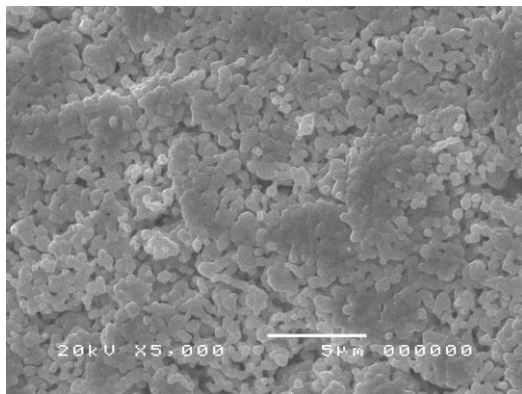
Figure 2: bright field micrograph (left), selected electron diffraction (saed, medium) along [010] direction and hr-tem images (right) of $\text{LaCo}_{0.5}\text{Fe}_{0.5}\text{O}_3$ ($R\bar{3}c$ space group).



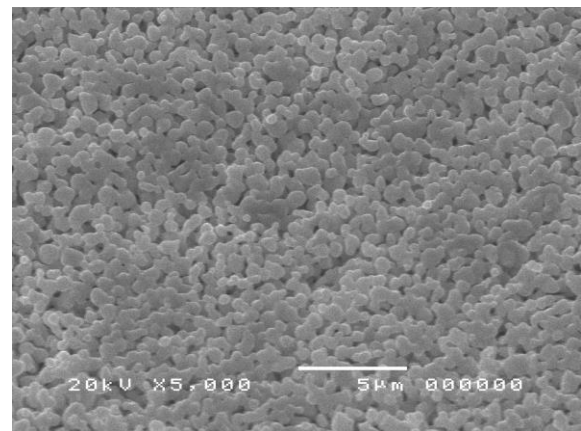
(c)



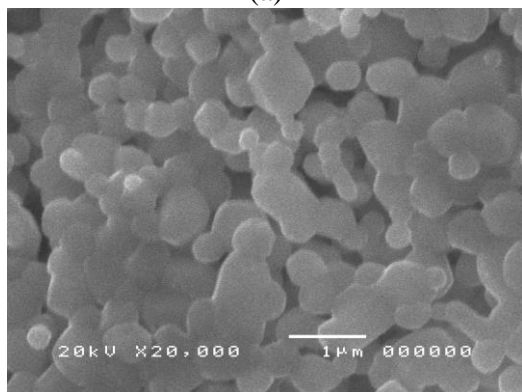
(d)



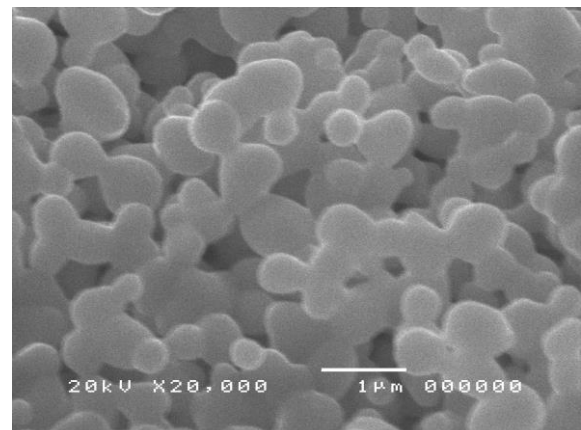
(a)



(e)



(b)



(f)

(f)

Figure 3: SEM images of top of the pellets of double-substituted perovskites sintered at 900 °C for 40 h:

$LaCo_{0.8}Fe_{0.1}Ni_{0.1}O_3$ (a, b),
 $LaCo_{0.8}Ti_{0.1}Ni_{0.1}O_3$ (c, d) and $LaCo_{0.8}Mn_{0.1}Fe_{0.1}O_3$ (e, f).

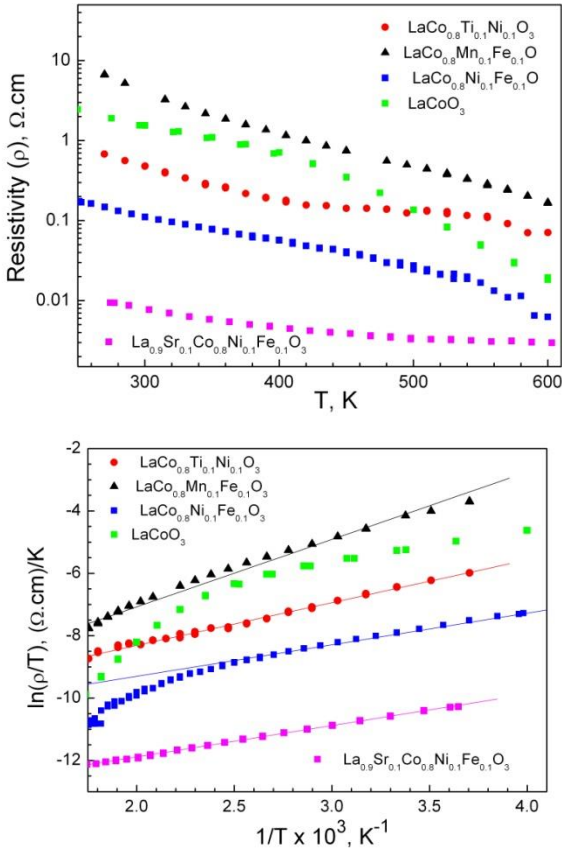


Figure 4 : Temperature dependence of the electrical resistivity, as well as the expression as “ $\ln(\rho/T)$ vs T^{-1} ” function, for unsubstituted $LaCoO_3$ and multiple substituted cobaltates.

It appears that the carrier mobility increases more rapidly with temperature for double substituted (Ni+Fe) and (Mn+Fe) cobaltates, while (Ni+Ti) and Sr-containing oxides have poor temperature dependence. As a result, at 600 K there is a tendency for equalization of carrier mobilities for all substituted perovskites. At 300 K, the carrier mobility decreases in the following order: Sr > (Ni+Ti) > (Mn+Fe) ≥ (Ni+Fe) ≈ $LaCoO_3$. It is deserve to note that Sr- and (Ni+Ti)-substituted cobaltates have both the higher carrier mobility (Fig. 5) and the lower extent of rhombohedral distortion (Table 1). This is an interesting result, which needs further examination.

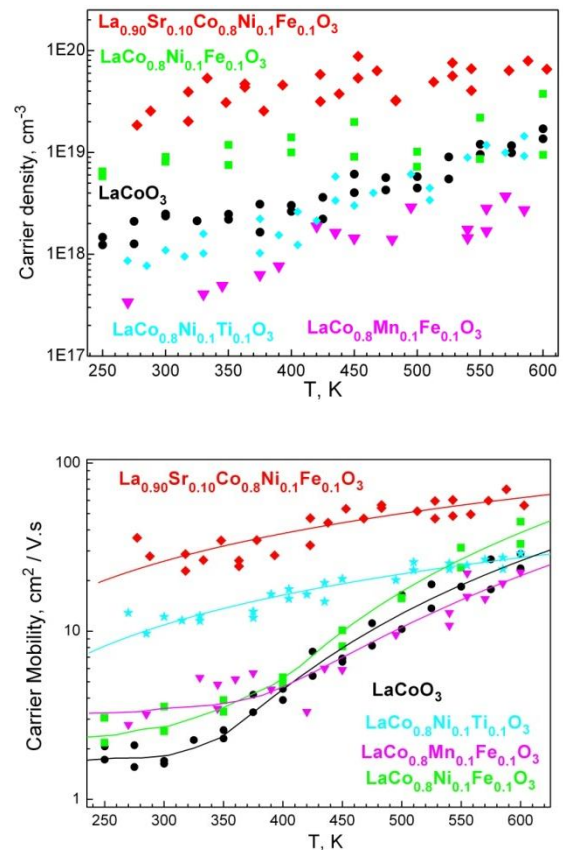


Figure 5: Temperature dependence of the carrier density (left) and carrier mobility (right) for unsubstituted $LaCoO_3$ and multiple substituted cobaltates $La_{0.9}Sr_{0.1}Co_{0.8}Ni_{0.1}Fe_{0.1}O_3$, $LaCo_{0.8}Ni_{0.1}Fe_{0.1}O_3$, $LaCo_{0.8}Ni_{0.1}Ti_{0.1}O_3$ and $LaCo_{0.8}Mn_{0.1}Fe_{0.1}O_3$.

The temperature dependence of the electrical resistivity, carrier density and mobility allow extracting three main conclusions. The enhanced electrical conductivity for Sr-substituted perovskite is a consequence from the increased carrier density and mobility, while the carrier density accounts only for the electrical conductivity of (Ni+Fe)- and (Mn+Fe)-substituted cobaltates. In the case of (Ni+Ti)-substituted perovskite, the reduction in the electrical resistivity versus that of $LaCoO_3$ is a result from the higher carrier mobility, which compensates the slight decrease in the carrier density.

For unsubstituted $LaCoO_3$, the temperature-induced spin crossover of Co^{3+} ions controls the electrical transport properties [5,21]. At 350 K it has been considered that both low- and high-spin states of Co^{3+} in equivalent amounts give rise to the electronic structure of $LaCoO_3$ and determine its short-range semiconductor behaviour [5]. By increasing the temperature, a gradual electronic delocalization takes place leading to an intermediate-

spin configuration of Co^{3+} ions (IS , $t_{2g}^5 e_g^1$), which are responsible for the stabilization of a metallic phase above 650 K. On the other hand, it has been suggested that the cobalt ions with an intermediate spin state (IS) start to form above 90K and the Jahn-Teller effect for the $t_{2g}^5 e_g^1$ configuration is mainly responsible for the semiconductor behavior of LaCoO_3 [22-24]. Finally, the appearance of IS configuration of Co ions in LaCoO_3 is not in agreement with the magnetic and thermal

expansion measurements of Asai *et al.* [25]. When metal ions substitute for A and B-perovskite sites, the temperature-induced spin crossover of Co^{3+} ions is changed depending on the nature of metal additives.

TABLE III.

ELECTRICAL RESISTIVITY, SEEBECK COEFFICIENT, POWER FACTOR ($\text{PF} = S^2 T / (\rho K_T)$), THERMAL CONDUCTIVITY, FIGURE OF MERIT ($\text{ZT} = S^2 T / (\rho K_T)$), POLARON HOPPING ENERGY (E_a), CARRIER MOBILITY, CARRIER DENSITY FOR $\text{La}_{1-y}\text{Sr}_y\text{Co}_{1-x}\text{M}_x\text{O}_3$ ($\text{M} = \text{Ni}, \text{Fe}; \text{Ti}, \text{Ni}; \text{Mn}, \text{Fe}$).

| Samples | ρ (290K), $\Omega \cdot \text{cm}$ | Seebeck coefficient, $\mu\text{V/K}$ | Power Factor, $\text{PF} = S^2 / \rho$ $\mu\text{W}/(\text{K}^2 \cdot \text{cm})$ | Thermal Conductivity, $\text{W}/(\text{m} \cdot \text{K})$ ± 0.04 | Figure of merit, $S^2 T / (\rho \cdot l)$ $T = 300 \text{ K}$ | E_a , eV | Mobility cm^2/Vs | Density $\text{cm}^{-3} \times 10^{18}$ |
|---|---|--|---|--|--|---------------|-------------------------------------|--|
| LaCoO_3 | 1.555 | 600 | 0.23 | 0.43 | 0.016 | ---- | 1.8 | 2.4 |
| $\text{LaCo}_{0.8}\text{Ni}_{0.1}\text{Fe}_{0.1}\text{O}_3$ | 0.062 | 234 | 0.88 | 0.17 | 0.156 | 0.093 | 2.7 | 8.6 |
| $\text{LaCo}_{0.8}\text{Ti}_{0.1}\text{Ni}_{0.1}\text{O}_3$ | 0.478 | 183 | 0.070 | 0.10 | 0.021 | 0.120 | 10.9 | 1.1 |
| $\text{LaCo}_{0.8}\text{Mn}_{0.1}\text{Fe}_{0.1}\text{O}_3$ | 2.631 | 46.6 | 0.0008 | 0.16 | 0.0002 | 0.190 | 3.5 | 0.4 |
| $\text{La}_{0.90}\text{Sr}_{0.10}\text{Co}_{0.8}\text{Ni}_{0.1}\text{Fe}_{0.1}\text{O}_3$ | 0.045 | 86 | 0.17 | 0.12 | 0.041 | 0.088 | 26.1 | 32.2 |

In LaCoO_3 , iron ions reduce the carrier density since they act as electron trapping centers, giving rise to electron localization in the cobaltates. In addition, it has been proposed that Fe^{3+} ions shift the spin transition of the cobalt ions to a higher temperature. Contrary to iron ions, the nickel ions give rise to electron delocalization. The interpretation of this fact is not easy task since nickel ions produce simultaneously an oxygen deficiency, an appearance of aliovalent Ni^{2+} ions (as charge compensators) and highly oxidized Co^{4+} ions. The occurrence of highly oxidized Co^{4+} ions is also observed when aliovalent Sr^{2+} ions substitute for La^{3+} ions in the A-perovskite site. It is interesting to note that the transport properties of $\text{LaCo}_{1-x}\text{Ni}_x\text{O}_3$ and $\text{La}_{1-x}\text{Sr}_x\text{CoO}_3$ are usually interpreted in the same manner, in which Co^{4+} ions play an important role for increasing the carrier density. The substitution of Ti^{4+} for Co^{3+} ions leads to an occurrence of Co^{2+} acting as electron donors, as a result of which there is a change in the carrier density. The substitution of manganese for cobalt in LaCoO_3 provokes a reaction of charge disproportion leading to stabilization of ions in mixed valence states: $\text{Mn}^{3+}\text{-Co}^{3+}$ and $\text{Mn}^{4+}\text{-Co}^{2+}$ ions [26]. Depending on the manganese content, the electrical resistivity decreases for slightly doped cobaltates ($x \leq 0.2$), followed by an

increase in the electrical resistivity for highly substituted cobaltates ($x > 0.2$) [26].

Irrespective of the fact that all transition metal ions substituted for Co ions are in equal amounts, the effect of Ni ions dominates over that of Fe and Ti ions leading to a reduction in the electrical resistivity of LaCoO_3 . Furthermore, the Sr^{2+} ions amplify the effect of electron delocalization, as a result of which a decrease in the electrical resistivity is strongest. In the case of (Mn+Fe)-double substitution, it appears that Fe ions have a dominant effect over that of Mn ions and an electrical resistivity increases.

Seebeck coefficient. As in the case of electrical resistivity, the Seebeck coefficient displays also a dependence on the nature of transition metal ions included in the perovskite structure (Table 3). The Seebeck coefficient (S) has a positive sign for all the perovskite compositions, thus indicating that the predominant mobile charge carriers are holes (Table 3). After the double substitution for cobalt ions, the Seebeck coefficient decreases, the lowest value being observed for (Mn+Fe)-containing cobaltates. It is notable that (Ni+Fe) and (Ni+Ti)-containing cobaltates have close values of the Seebeck coefficient irrespective of the fact

that they display big difference in their electrical resistivity. Further decreases in the Seebeck coefficient is achieved when aliovalent Sr^{2+} ions substitute for La^{3+} ions.

Cobaltates known as strongly correlated electron systems exhibit large thermopower, that can be calculated taking into account the carrier concentration (x) and the ratio of the spin and orbital degeneracy for both electron donor and electron acceptor sites (g_I/g_{II}): $S = -k_B/e \ln[(g_I/g_{II})\{(1-x)/x\}]$ where k_B is the Boltzmann constant and e is the elementary electric charge [27]. This means that the higher is the charge carrier concentration; the lower is the magnitude of the thermopower. In addition, cobalt ions in the LaCoO_3 -system adopt mixed valence states with two different electronic configurations (such as $\text{Co}^{3+}/\text{Co}^{4+}$ and/or $\text{Co}^{2+}/\text{Co}^{3+}$), which are mainly responsible for the electronic degeneracy. This approach can be used in order to rationalize the dependence of the thermopower on the nature of metal ions substituted for La^{3+} and Co^{n+} ions. Since the hole conductivities account mainly for the electrical transport properties of all multiple-substituted perovskites, then the dependence of S on the nature of the metal ions can simply be described by the observed changes in the carrier density. Thus, the decrease in the magnitude of S for (Ni+Fe) and Sr/(Ni+Fe)-containing cobaltates is related with increased density of charge carriers (Fig. 5). This result confirms once again that Ni and Sr ions play a dominant role in the thermoelectric activities of multiple substituted cobaltates. It is worth to mention that the transport properties of $\text{LaCo}_{1-x}\text{Ni}_x\text{O}_3$ and $\text{La}_{1-x}\text{Sr}_x\text{CoO}_3$ are usually interpreted in the same manner by taking into account the contribution of highly oxidized Co^{4+} ions [28-30].

The dependence of S on the carrier density is also demonstrated by its temperature evolution (Fig. 6). The Seebeck coefficient decreases with increasing the recording temperature, while the carrier density increases in the same order.

For (Ni+Ti) and (Mn+Fe)-double substituted cobaltates having lower density of charge carriers, one can expect an increase in the magnitude of S . However, a significant decrease in S is observed. This discrepancy means that the electronic degeneracy plays an important

role in the magnitude of the thermopower for (Ni+Ti) and (Mn+Fe)-double substituted cobaltates. The result can be related with a possible occurrence of Co^{2+} ions in both (Ni+Ti)- and (Mn+Fe)-containing compositions instead of highly oxidized Co^{4+} ions. This is in agreement with early proposed electronic structure for single substituted $\text{LaCo}_{1-x}\text{Ti}_x\text{O}_3$ and $\text{LaCo}_{1-x}\text{Mn}_x\text{O}_3$.

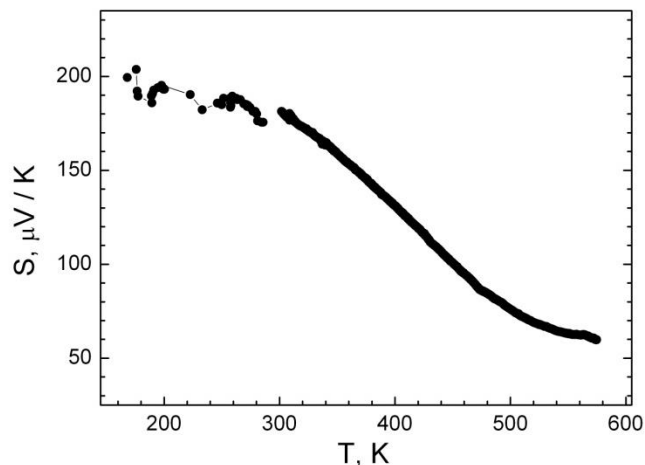


Figure 6 : Temperature dependence of the Seebeck coefficient (S) for $\text{LaCo}_{0.8}\text{Ni}_{0.1}\text{Ti}_{0.1}\text{O}_3$.

Thermal conductivity: The thermal conductivity is the next parameter that is strongly affected by the presence of Ni, Fe, Mn, Ti and Sr ions in the perovskite structure (Table 3). The comparison shows that the thermal conductivity decreases upon metal substitution (Table 3). The results do not show any measurable dependence on the nature of metal ions substituted for La or Co-ions.

For cobaltates, the thermal conductivity can be expressed by two terms due to the electronic and lattice contributions. Assuming one type of charge carriers contributing to electron conduction, the electronic contribution to the thermal conductivity can be related with electrical resistivity: λ_e can be calculated by the: $\kappa_e = LT/\rho$ (Wiedemann-Franz law, L is the Lorentz number of $2.45 \times 10^{-8} \text{ V}^2 \text{ K}^{-2}$). It is obvious that the κ_e term increases for more conductive perovskites ($4 \cdot 10^{-4}$, 0.010 , 0.0015 , $3 \cdot 10^{-4}$ and $0.016 \text{ W}/(\text{m}\cdot\text{K})$ for LaCoO_3 and (Ni+Fe), (Ni+Ti), (Mn+Fe) and Sr-containing cobaltates, respectively), but it remains lower than the total thermal conductivity (0.43 , 0.17 , 0.10 , 0.16 and $0.12 \text{ W}/(\text{m}\cdot\text{K})$, respectively). This means that the total thermal conductivity for all the substituted perovskites is governed by the lattice contribution. The dopant-induced

decrease in the thermal conductivity can be understood by the enhancement of phonon scattering due to the disordering of metal ions in the octahedral Co-position (with coordinates 0, 0, 0) of the perovskite structure. This is a consequence of the ionic mismatch of the nickel, iron, titanium, manganese and cobalt ions (Table 1).

Figure of merit: Taking into account the Seebeck coefficient and electrical resistivity data, the power factor is calculated: $PF=S^2/\rho$ (Table 3). It appears that PF is highest for (Ni+Fe)-double substituted LaCoO_3 , while both (Ni+Ti) and (Mn+Fe)-additives cause a decrease in PF . The PF of Sr-containing cobaltates is close to that of unsubstituted LaCoO_3 . It is worth to mention that observed power factor for multiple-substituted cobaltates is lower in comparison with than of SrTiO_3 , which is reported as the highest power factor for oxides ($20 \mu\text{W}/(\text{K}^2.\text{cm})$) [31,32]. However, the extremely large thermal conductivity of SrTiO_3 (about $10 \text{ W}/(\text{m.K})$) reduces its figure of merit [32,33].

Taking into account the thermal conductivity in addition to power factor, the figure of merit is improved (Table 3). This improvement is more significant for (Ni+Fe)-substituted cobaltates (more than one order). The reduced thermal conductivity leads to a higher magnitude of the figure of merit even for (Ni+Ti)- and Sr-containing oxides. Among multiple-substituted cobaltates, only the (Mn+Fe) pair has a negative effect on thermoelectric properties of cobaltates.

IV. CONCLUSION

The substitution for Co with $(\text{Ni}_{0.10}\text{Fe}_{0.10})$, $(\text{Ni}_{0.10}\text{Ti}_{0.10})$ and $(\text{Mn}_{0.10}\text{Fe}_{0.10})$ pairs proceeds by preservation of the rhombohedral perovskite structure of LaCoO_3 . The occurrence of (Mn+Fe) and (Ni+Fe) pairs into $\text{LaCo}_{0.8}\text{M}_{0.1}\text{M}'_{0.1}\text{O}_3$ causes an elongation of the mean bond lengths $\text{La-Co}_{0.8}\text{M}_{0.1}\text{M}'_{0.1}$ and $\text{Co}_{0.8}\text{M}_{0.1}\text{M}'_{0.1}\text{O}$ without changing the extent of rhombohedral distortion of metal octahedra, while the (Ti+Ni) pair reduces significantly the local rhombohedral distortion together with an increase of the mean $\text{La-Co}_{0.8}\text{M}_{0.1}\text{M}'_{0.1}$ bond distance. Further reduction in the extent of the rhombohedral distortion is achieved by replacement of La^{3+} with Sr^{2+} ions.

Double substituted cobaltates are semiconductors with hole conductivities. The carrier density increases after $(\text{Ni}_{0.10}\text{Fe}_{0.10})$ double substitution for Co ions, as well as after the replacement of La^{3+} with Sr^{2+} ions. The enhancement of the carrier density of multiple substituted perovskites is related with the appearance of highly oxidized Co^{4+} ions as charge compensators. When $(\text{Ni}_{0.10}\text{Ti}_{0.10})$ and $(\text{Mn}_{0.10}\text{Fe}_{0.10})$ pairs substitute for Co^{3+} ions, there is a decrease in the carrier density of cobaltates $\text{LaCo}_{0.8}\text{M}_{0.1}\text{M}'_{0.1}\text{O}_3$, which is a consequence of the appearance of electron trapping centres such as low-oxidized Co^{2+} ions. The carrier mobility depends on the extent of the rhombohedral distortion: the higher is the distortion, the lower is the mobility.

The simultaneous changes in the carrier density and the carrier mobility are responsible for the observed variation in the Seebeck coefficient: S decreases for multiple substituted perovskites. The structural disorder induced by ionic mismatch of the nickel, iron, titanium, manganese and cobalt ions is responsible for the effective decrease in the thermal conductivity of multiple substituted perovskites.

The power factor is strongly dependent on the origin of metal substituents. The highest PF is observed for (Ni+Fe)-double substituted LaCoO_3 , while both (Ni+Ti) and (Mn+Fe)-additives cause a decrease in PF . The Sr-containing cobaltates displays a power factor close to that of unsubstituted LaCoO_3 .

The reduced thermal conductivity for multiple substituted perovskites determines their improved thermoelectric efficiency: the highest figure of merit is reached for (Ni+Fe)-double substituted LaCoO_3 . Among multiple-substituted cobaltates, only the (Mn+Fe) pair has a negative effect on thermoelectric properties of cobaltates.

This study demonstrates clearly that by a rational choose of metal ions it is possible to control the thermopower efficiency of cobaltates in respect of their desired applications.

V. ACKNOWLEDGEMENTS

Authors are grateful to the financial support from ESF (Grant BG051PO001-3.3.06-0050).

VI. REFERENCES

- [1] Sootsman, J.R., Chung, D.Y., and Kanatzidis, M.G. 2009. New and old concepts in thermoelectric materials, *Angew. Chem., Int. Ed.*, 48, 8616–8639, DOI: 10.1002/anie.200900598.
- [2] Yan, J., Gorai, P., Ortiz, S., Miller, B., Barnett, S.A., Mason, T., Stevanović, V., and Toberer, E.S. 2015. Material descriptors for predicting thermoelectric performance. *Energy Environ. Sci.*, 8, 983-994, DOI: 10.1039/C4EE03157A.
- [3] Terasaki, I., Sasago, Y., Uchinokura, K., 1997. Large Thermoelectric Power in NaCo_2O_4 Single Crystals. *Phys. Rev. B* 56, R12685-R12687, DOI: <https://doi.org/10.1103/PhysRevB.56.R12685>.
- [4] Hébert, S., Kobayashi, W., Muguerra, H., Bréard, Y., Ragavendra, N., Gascoin, F., Guilmeau, E., and Maignan, A. 2013. From oxides to selenides and sulfides: The richness of the CdI_2 type crystallographic structure for thermoelectric properties. *Phys. Status Solidi a* 210, 69-81, DOI: 10.1002/pssa.201228505.
- [5] Señarís Rodríguez, MA, Goodenough, J.B., 1995. LaCoO_3 Revisited. *J. Solid State Chem.*, 116, 224-231, DOI: 10.1006/jssc.1995.1207.
- [6] Berggold, K., Kriener, M, Zobel, C., Reichl, A., Reuther, M., Müller, R., Freimuth, A. and Lorenz, T. 2005. Thermal conductivity, thermopower, and figure of merit of $\text{La}_{1-x}\text{Sr}_x\text{CoO}_3$. *Phys. Rev. B* 72, 155116, DOI: 10.1021/jp105367r.
- [7] Herve, P., Ngamou, T. and Bahlawane, N. 2010. Influence of the Arrangement of the Octahedrally Coordinated Trivalent Cobalt Cations on the Electrical Charge Transport and Surface Reactivity. *Chem. Mater.* 22, 4158-4165, DOI: 10.1021/cm1004642.
- [8] Yu, J., Kamazawa, K., and Louca, D. 2010. Nature of magnetoelastic coupling with the isovalent substitution at the B-site in $\text{LaCo}_{1-y}\text{B}_y\text{O}_3$. *Phys. Rev. B* 82, 224101, DOI: 10.1103/PhysRevB.82.224101.
- [9] Wang, Y., Li, F., Xu, L., Sui, Y., Wang, X., Su, W., and Liu, H. 2011. Large thermal conductivity reduction Induced by La/O Vacancies in the Thermoelectric LaCoO_3 System. *Inorg. Chem.* 2011, 50, 4412–4416, DOI: 10.1021/ic200178x.
- [10] Vulchev, V., Vassilev, L., Harizanova, S., Khristov, M., Zhecheva, E. and Stoyanova, R. 2011. Improving of the thermoelectric efficiency of LaCoO_3 by double substitution with nickel and iron. *J. Phys. Chem. C* 116, 13507–13515, DOI: 10.1021/jp3021408.
- [11] Harizanova S., Zhecheva, E., Valchev, V., Khristov, M., Stoyanova, R., 2015. Improving the thermoelectric efficiency of co based ceramics. *Materials Today: Proceedings* 2, 4256, DOI: 10.1016/j.matpr.2015.09.011.
- [12] Ivanova, S., Senyshyn, A., Zhecheva, E., Tenchev, K., Stoyanova, R., Fuess, H., 2010. Crystal structure, microstructure and reducibility of $\text{LaNi}_x\text{Co}_{1-x}\text{O}_3$ and $\text{LaFe}_x\text{Co}_{1-x}\text{O}_3$ Perovskites ($0 < x < 0.5$). *J. Solid State Chem.* 183, 940-950. DOI:10.1016/j.jssc.2010.02.009
- [13] Schulz, B. 1981. Thermal conductivity of porous and highly porous materials, *High Temp. High Press.* 13, 649–660, ISSN 0018-1544.
- [14] Zuev, A.Yu., Vylkov, A.I., Petrov, A.N., and Tsvetkov, D.S. 2008. Defect structure and defect-induced expansion of undoped oxygen deficient perovskite $\text{LaCoO}_{3-\delta}$. *Solid State Ionics* 179, 1876-1879, DOI: 10.1016/j.ssi.2008.06.001.
- [15] Mastin, J., Einarsrud, M.A. and Grande T. 2006. Structural and Thermal Properties of $\text{La}_{1-x}\text{Sr}_x\text{CoO}_{3-\delta}$. *Chem. Mater.* 18, 6047–6053, DOI: 10.1021/cm061539k.
- [16] Kozuka, H., Ohbayashi, K., and Koumoto, K. 2015. Electronic conduction in La-based perovskite-type oxides. *Sci. Technol. Adv. Mater.* 16, 026001, DOI: 10.1088/1468-6996/16/2/026001
- [17] Alonso, J.A., Martínez-Lope, M.J., Casais, M.T., Macmanus-Driscoll, J.L., de Silva, P. S. I. P. N., Cohen, L.F. and Fernández-Díaz, M.T. 1997. Non-stoichiometry, structural defects and properties of $\text{LaMnO}_{3+\delta}$ with high δ values ($0.11 \leq \delta \leq 0.29$). *J. Mater. Chem.* 7, 2139-2144, DOI: 10.1039/A704088A.
- [18] Matsumoto, G. 1970. Study of $(\text{La}_{1-x}\text{Ca}_x)\text{MnO}_3$. I. Magnetic Structure of LaMnO_3 . *J. Phys. Soc. Jpn.* 29, 606-615, DOI: 10.1143/JPSJ.29.606.
- [19] Elemans, J.B.A.A., Laar, B.V., Veen, K.R.V.D., and Loopstra, B.O. 1971. The crystallographic and magnetic structures of $\text{La}_{1-x}\text{Ba}_x\text{Mn}_{1-x}\text{Me}_x\text{O}_3$ (Me

- = Mn or Ti). *J. Solid State Chem.* 3, 238-242, DOI:10.1016/0022-4596(71)90034-X.
- [20] Troyanchuk, I.O., Karpinsky, D.V., Szymczak, R., and Szymczak, H. 2006. Effect of oxygen deficit on magnetic properties of $\text{LaCo}_{0.5}\text{Fe}_{0.5}\text{O}_3$. *J. Magn. Magn. Mater.* 298, 19-24, DOI: 10.1016/j.jmmm.2005.03.009.
- [21] Sehlin, S. R., Anderson, H. U., and Sparlin, D. M., 1995. Semiemperila model for the electrical properties of $\text{La}_{1-x}\text{Ca}_x\text{CoO}_3$. *Phys. Rev. B*, 52, 11681, DOI: 10.1103/PhysRevB.52.11681.
- [22] Korotin, M. A., Ezhov, S, Solovyev, Yu, IV, Anisimov, V. I., Khomskii, D. I., and Sawatzky, G. A., 1996. Intermediate-spin state and properties of LaCoO_3 . *Phys. Rev. B*, 54, 5309-5316, DOI: /10.1103/PhysRevB.54.5309.
- [23] Yamaguchi, S., Okimoto, Y., and Tokura, Y., 1997. Local lattice distortion during the spin-state transition in LaCoO_3 . *Phys. Rev. B*, 55, R8666-R8669, DOI: <https://doi.org/10.1103/PhysRevB.54.5309>.
- [24] Saitoh, T., Mizokawa, T., Fujimori, A., Takeda, Y., and Takano, M., 1999. Strontium-doped Lanthanum Cobalt Oxides Studied by XPS. *Surf. Sci. Spectra*, 6, 302-312, DOI: 10.1116/1.1247936.
- [25] Asai, K., Yoneda, A., Yokokura, O., Tranquada, J. M., Shirane, G., and Kohn, K., 1998. Two Spin-State Transitions in LaCoO_3 . *J. Phys. Soc. Jpn.*, 67, 290-296, DOI: 10.1143/JPSJ.67.290.
- [26] Narasimhan, V., Keer, H.V., and Chakrabar, D.K. 1985. Structural and Electrical Properties of the $\text{LaCo}_{1-x}\text{Mn}_x\text{O}_3$ and $\text{LaCo}_{1-x}\text{Fe}_x\text{O}_3$ Systems, *Phys. Stat. Sol. (a)* 89, 65-71. DOI: 10.1002/pssa.2210890105.
- [27] Koshibae, W., Tsutsui, K., Maekawa, S., 2000. Thermopower in cobalt oxides. *Phys. Rev. B*, 62, 6869-6872, DOI: <https://doi.org/10.1103/PhysRevB.62.6869>.
- [28] Kyômen, T., Yamazaki, R., and Itoh, M., 2003. Valence and spin state of Co and Ni ions and their relation to metallicity and ferromagnetism in $\text{LaCo}_{0.5}\text{Ni}_{0.5}\text{O}_3$. *Phys. Rev. B*, 68, 104416, DOI: <https://doi.org/10.1103/PhysRevB.68.104416>.
- [29] Androulakis, J., Katsarakis, N., Viskadourakis, Z., and Giapintzakis, J., 2003. Comparative study of the magnetic and magnetotransport properties of a metallic and a semiconducting member of the solid solution $\text{LaNi}_x\text{Co}_{1-x}\text{O}_3$. *J. Appl. Phys.*, 93, 5484-5490, DOI: 10.1063/1.1561589.
- [30] Viswanathan, M., Anil Kumar PS., 2009. Observation of reentrant spin glass behavior in $\text{LaCo}_{0.5}\text{Ni}_{0.5}\text{O}_3$. *Phys. Rev B*, 80, 012410-1-012410-4, DOI: <https://doi.org/10.1103/PhysRevB.80.012410>.
- [31] Chen, R., Delgado, R. D., Garnett, E. C., Hochbaum, A. I., Liang, W., Majumdar, A., Najarian, M., and Yang, P., 2008. Enhanced thermoelectric performance of rough silicon nanowires. *Nature*, 451, 163-168 DOI: 10.1038/nature06381.
- [32] Chateigner, D., Chong, K., Funahashi, R., Guilmeau, E., and Mikami, M. 2004. Thermoelectric properties–texture relationship in highly oriented $\text{Ca}_3\text{Co}_4\text{O}_9$ composites. *Appl. Phys. Lett.*, 85, 1490-1492, DOI: 10.1063/1.1785286.
- [33] Yadav, G. G., Zhang, G., Qiu, B., Susoreny, J. A., Ruan, X., and Wu, Y., 2011. Synthesis and Thermoelectric Properties of Compositional Modulated Lead Telluride–Bismuth Telluride Nanowire Heterostructures. *Nanoscale*, 3, 4078–4081, DOI: 10.1021/nl400319u.